1963) [Translated into English (New York: Consultants Bureau, 1964)]

19. Keldysh L V, Doctoral Thesis (Moscow: P N Lebedev Physics Inst., USSR Acad. of Sciences, 1965)

20. Zakharov A L *Zh. Eksp. Teor. Fiz.* **38** 665 (1960) [*Sov. Phys. JETP* **11** 478 (1960)]

21. Aleksandrov A S, Elesin V F *Zh. Eksp. Teor. Fiz.* **58** 1067 (1970) [*Sov. Phys. JETP* **31** 571 (1970)]

22. Adams E N, Holstein T D *J. Phys. Chem. Solids* **10** 254 (1959)

# Magnetoimpurity resonances as indicators of an inverse photoelectron distribution function in semiconductors

V F Gantmakher, V N Zverev

The mechanism of absolute negative conductivity, due to the specific way in which electrons behave in crossed electric and quantizing magnetic fields, was predicted by Elesin in 1968 [1] and observed experimentally by Aleksandrov et al. [2]. According to Ref. [1], because the magnetic subband density of states $g(\varepsilon) \sim \varepsilon^{-1/2}$ is a decreasing function of energy, an electron which is far enough above the bottom of a subband tends to gain potential energy at the expense of its kinetic energy when elastically (or quasi-elastically) scattered in collisions. The energy conservation law for such collisions is

$$eE\Delta X + \Delta\varepsilon \pm u = 0 , \qquad (1)$$

where the first two terms are the respective changes in the electron potential and kinetic energies, $\Delta X$ is the shift in the position of the Larmor orbit center, and $u$ is the energy of the absorbed (emitted) acoustic phonon. (The term $u$ in Eqn (1) is added for phonon scattering, for which the quasi-elasticity condition is expressed by the inequality $\varepsilon \gg u$.)

For electrons with energy $\varepsilon > eE\Lambda$ the average value of $eE\Delta X$ is positive. For an equilibrium distribution function, this negative contribution to the conduction is compensated by the positive contribution from the electrons in the energy range $\varepsilon \leqslant eE\Lambda$ close to the subband bottom. But if such near-bottom electrons are too few for some reason, then in the presence of a strong magnetic field and a perpendicular electric field the total conductivity of this group of carriers may prove negative.

In the experiment in Ref. [2], non-equilibrium electrons were produced by interband monochromatic photoexcitation in the direct-band-gap semiconductor p-InSb at helium temperatures. Because the lifetime of the photoelectrons was much shorter than the characteristic energy relaxation time, the electron distribution function turned out to be quite far from equilibrium and was determined by the line shape of the light source used. Therefore, any time electrons were created close to the edges of the magnetic subbands, the photocurrent spectrum exhibited a negative minimum, due to the absolute negative conductivity effect.

A necessary but clearly not sufficient condition for absolute negative conductivity to occur is that there be a region in which the distribution function has a positive derivative, $\partial f/\partial\varepsilon > 0$. This point seems to have been first made in the theoretical work of Ref. [3], in which the

cyclotron resonance response in the conductivity of semiconductors with negative effective masses was investigated. For low-frequency transport, in electric and magnetic crossed fields the easiest way to show this is by means of a model which describes exchange processes in an electronic system in terms of electron diffusion in energy space [4, 5]. In this model, the energy obtained from the electric field, $(\partial U/\partial t)_E$, is given by

$$\left(\frac{\partial U}{\partial t}\right)_E = -\int_0^\infty D_\varepsilon \frac{\partial f}{\partial\varepsilon} g \, d\varepsilon , \qquad (2)$$

where $D_\varepsilon$, the diffusion coefficient along the $\varepsilon$-axis, is determined by how far the center of the Larmor orbit shifts in collisions [5]. From Eqn (2) it is seen that the inequality $(\partial U/\partial t)_E < 0$ can only be satisfied if there is a region where $\partial f/\partial\varepsilon > 0$. In addition, it can be seen that for a given function $f(\varepsilon)$ integral (2) can be positive for one function $D_\varepsilon$ (i.e., for one type of scatterers) and negative for another.

Absolute negative conductivity mechanisms for inelastic processes in two-dimensional systems were analyzed theoretically by Ryzhiĭ [6], whose predictions were to wait 30 years before being experimentally realized. Relatively recently, zero-resistance states were discovered in samples of 2D high electron mobility GaAs/AlGaAs heterostructures subjected to strong microwave radiation [7]. In describing this phenomenon, current models [8] are all to a greater or lesser extent based on the mechanism of absolute negative conductivity — an effect due to a strong non-equilibrium which microwave radiation produces in the electron distribution function [1, 6].

Experiments on heterostructures renewed interest in the subject, and it seems therefore appropriate here to revisit our old experiments on low-temperature magnetotransport in photoexcited germanium doped with shallow acceptor impurities [9]. As part of that work, a study of magnetoimpurity oscillations was carried out, which showed that conductivity in crossed electric and quantizing magnetic fields has a negative part, due to the distortion of the photoelectron distribution function. The magnetoimpurity oscillations look like a sequence of photocurrent peaks periodic in an inverse magnetic field (Fig. 1), which are due to inelastic
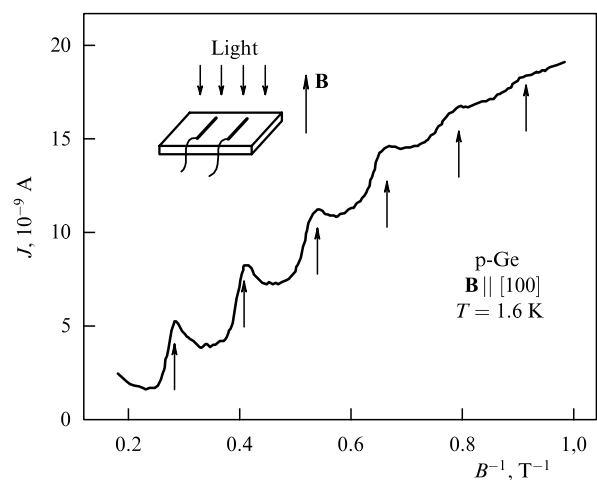


**Figure 1.** Magnetoimpurity oscillations of photoconductivity in a sample of gallium-doped p-Ge. $N_{\mathrm{Ga}} = 2 \times 10^{14}$ cm$^{-3}$, the pulling field $E = 3.5$ V cm$^{-1}$, interband generation rate $G = 10^{17}$ cm$^{-3}$ s$^{-1}$, light wavelength $\lambda = 0.63$ μm.
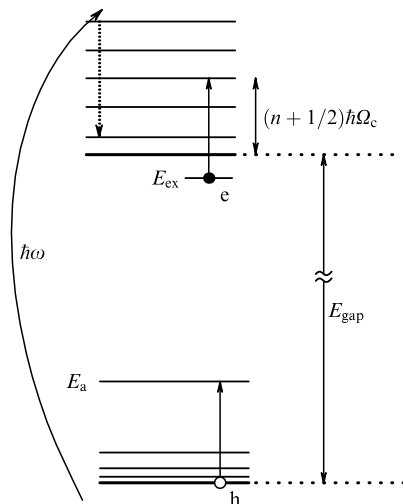
**Figure 2.** Energy diagram illustrating the decay of an ionized acceptor exciton — an elementary inelastic scattering process leading to magneto-impurity oscillations in p-Ge.
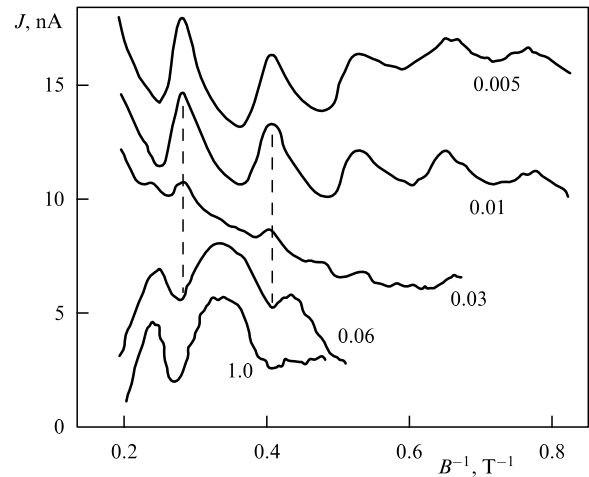


**Figure 3.** Inversion of photoconductivity oscillations in p-Ge with variation in interband photoexcitation intensity. Numbers at the curves are the values of the generation rate $G$ in units of $10^{20}$ $cm^{-3}\,s^{-1}$; $T = 1.5$ K, the pulling field $E = 3.5$ V $cm^{-1}$. Here and below the monotonic part of $J(B^{-1})$ is compensated.

scattering resonances occurring when the Landau level separation is equal to the characteristic energy of the impurity centers. Inelastic scattering resonance processes are quite diverse, as are the characteristic energies they involve [10]. In particular, in p-Ge the decay of ionized acceptor excitons is a resonance process [11] — an Auger-type one (Fig. 2) in which a hole makes a transition to the ground state level of an acceptor, whereas an electron goes to the conduction band with excess energy $\Delta\varepsilon = E_a - E_{ex}$, the difference between the acceptor and exciton binding energies in germanium. In a quantizing magnetic field, ionized acceptor excitons decay resonantly with respect to the magnetic field, i.e., the decay probability increases sharply each time the electron occupies a Landau level. At the resonance

$$\hbar\Omega_c(n + 1/2) = \Delta\varepsilon, \quad n = 1, 2, \ldots, \qquad (3)$$

(where $\Omega_c = eB/m^*c$ is the electron cyclotron frequency), implying that the oscillations are periodic in the inverse magnetic field with period $P_{1/B} = e\hbar/m^*c\Delta\varepsilon$ dependent on the characteristic energy transfer to an electron in an inelastic process, $\Delta\varepsilon \approx \Delta\varepsilon(0) = E_a(0) - E_{ex}(0)$. Note that the linear term in the magnetic field in $\Delta\varepsilon(B)$ and the $1/2$ term on the right-hand side of Eqn (3) do not affect the period of oscillation and only lead to a phase shift on the $1/B$ scale, whereas the nonlinear terms are small and virtually do not violate the periodicity of the oscillations.

As seen from the table, the characteristic energies $\Delta\varepsilon$ obtained from the period of magnetoimpurity oscillations in samples with different acceptor impurities agree very closely with the corresponding values of $[E_a(0) - E_{ex}(0)]$ known from spectroscopic measurements. Although the observed

oscillatory resonances were initially given other explanations, it was mainly these coincidences which led to the conclusion that the observed oscillations are exactly due to resonantly decaying ionized acceptor excitons [11, 12]. Special experiments under pressure also confirmed this conclusion [13].

For all of the complexity of the non-equilibrium system under study — which includes non-equilibrium holes and excitons and neutral and ionized acceptors along with electrons — the key point of change at a resonance is an increase in the concentration of non-equilibrium electrons, which is exactly what shows up in the form of photocurrent peaks (see Fig. 1). This resonant behavior persists over a wide range of the interband generation rate $G$ — until, as $G$ increases, the oscillations are inverted and their peaks become troughs as seen in Fig. 3. Reference [9], where we report the discovery of the inversion of magnetoimpurity
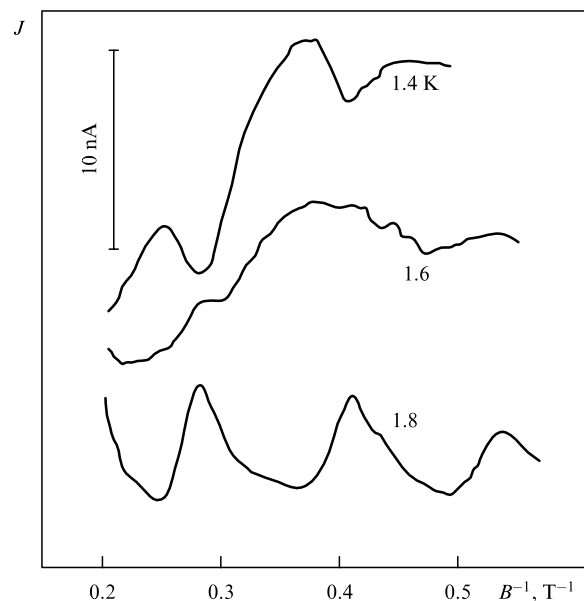
**Table.**

| Acceptor | $\Delta\varepsilon$, meV | $E_a - E_{ex}$, meV |
|----------|--------------------------|---------------------|
| In       | 7.5                      | 7.57                |
| Ga       | 6.85                     | 6.92                |
| B        | 6.25                     | 6.42                |



**Figure 4.** Inversion of photocurrent oscillations with variation in temperature; $G = 2 \times 10^{18}$ $cm^{-3}\,s^{-1}$, the pulling field $E = 5$ V $cm^{-1}$.
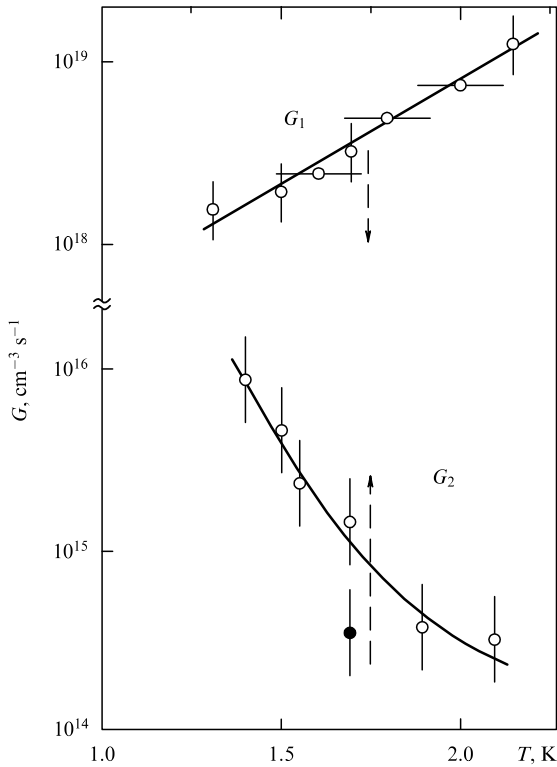
**Figure 5.** Relation between the oscillation inversion values of $G$ and $T$. Circles with vertical bars are obtained from a series of curves with different $G$ and $T = $ const, and circles with horizontal bars from a series of curves with different $T$ and $G = $ const. Curve $G_1(T)$ was obtained for $E = 5$ V cm$^{-1}$. For larger $E$, it starts to move in the direction indicated by the arrow. Curve $G_2(T)$ is obtained for $E = 7$ V cm$^{-1}$. Its shift with the field is also indicated by an arrow. Closed circle: $E = 5$ V cm$^{-1}$.

oscillations, also contains a detailed study of the effect. It was established that the inversion arises in the generation rate range $10^{18} - 10^{19}$ cm$^{-3}$ s$^{-1}$ and that it is observed not only when $G$ is changed but also when the temperature is changed (Fig. 4). The critical values of $G_1$ and $T$ are related to each other in that the higher $T$ is the larger the generation rate $G_1$ at which the inversion takes place (see the upper curve in Fig. 5).

By measuring the temperature dependence of the photocurrent $J(T)$ at a fixed magnetic field, it was possible to establish a correlation between the inversion moment of the magnetoimpurity oscillations of photocurrent on the one hand and the nature of the $J(T)$ dependence on the other. The inversion occurs at the same values of $T$ and $G$ at which the curves $J(T)$ exhibit kinks that separate regions of weak and strong temperature dependence of the photocurrent (Fig. 6). In regions where the photocurrent is practically independent of temperature, the resonances have the form of troughs, and in regions where it increases strongly with increasing temperature, they have the form of peaks.

As the generation rate decreases below $G_1$, the relative oscillation amplitude $A$ slightly increases at first, reaching a maximum at values of $G$ lying in the range from $2 \times 10^{16}$ to $2 \times 10^{17}$ cm$^{-3}$ s$^{-1}$ depending on the sample. Upon further decrease in the generation rate the value of $A$ decreases, and the oscillations disappear at $G \approx 10^{15} - 10^{14}$ cm$^{-3}$ s$^{-1}$.

Such $A(G)$ dependence occurs only at small enough electric fields $E$. At low generation rates, however, even a relatively small increase in the field $E$ led again to inverted
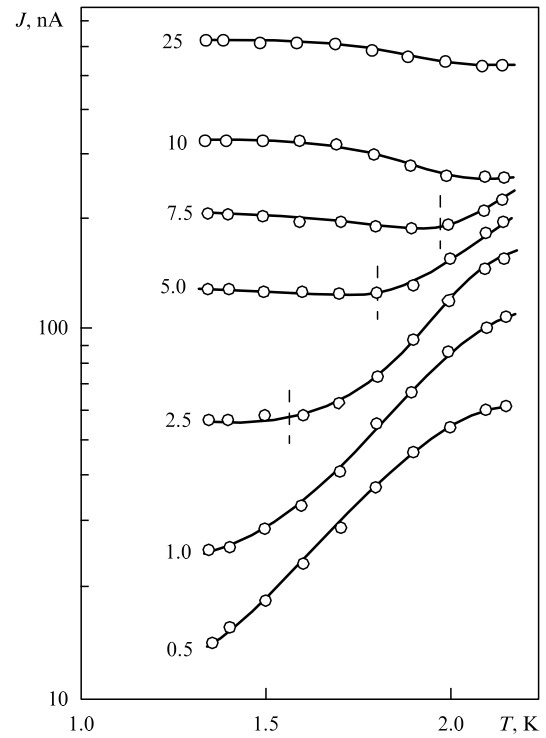


**Figure 6.** Temperature dependence of photocurrent at different generation rates. Numbers at the curves indicate the values of $G$ in units of $10^{18}$ cm$^{-3}$ s$^{-1}$; $B = 28.5$ kOe, $E = 5$ V cm$^{-1}$. Vertical bars indicate the temperatures at which inversion takes place at the corresponding value of $G$.

oscillations as shown in Fig. 7. The curve $G_2(T)$ in Fig. 5 depicts the onset of this second inversion. As $E$ decreases, $G_2(T)$ shifts downward and levels off to a value at which the oscillations disappear (i.e., at small $E$ the oscillations disappear without undergoing inversion). The upward shift of the $G_2(T)$ curve with increasing $E$ is limited: for
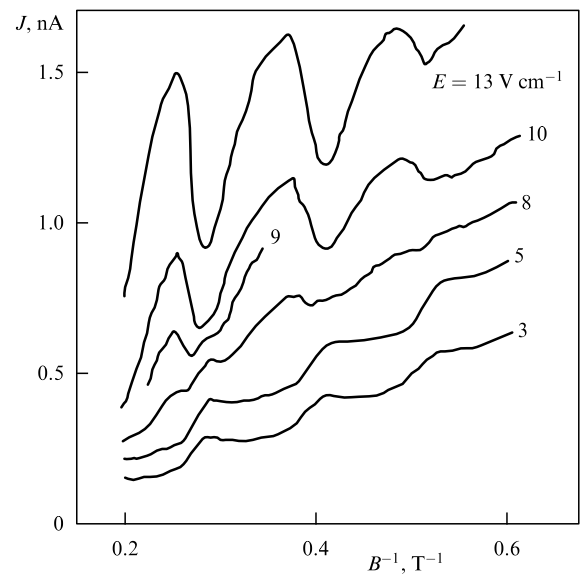


**Figure 7.** Inversion of photocurrent oscillations with variation in electric field strength in the region of low generation rates; $G = 6 \times 10^{15}$ cm$^{-3}$ s$^{-1}$, $T = 1.4$ K.

$G \approx 10^{17}$ cm$^{-3}$ s$^{-1}$, the electric field produces no inversion at all, and the photocurrent peaks at the resonances persist all the way to the low-temperature breakdown. Finally, at still higher values of $G$ (but somewhat less than $G_1$), the electric field again stimulates inversion, shifting the $G_1(T)$ curve downward. In practical terms, this shift is noticeable in a field on the order of 10 V cm$^{-1}$.

Thus, increasing the electric field leads to inverted oscillations at low and high values of the generation rate $G$; at intermediate values of $G$ the magnetoimpurity resonances maintain the form of peaks even though the electronic system is undoubtedly heated — leading even to a low-temperature breakdown.

In the discussion below the following points hold. All carriers in our experiments are photocarriers, the equilibrium electron and hole concentrations being negligibly small at helium temperatures. Electrons with energies greater than the optical phonon energy do not play an important role in kinetics because both the total diffusion coefficient along the magnetic field $B$ and the total mobility perpendicular to $B$ are determined by less energetic electrons. And finally, the carriers are distributed uniformly throughout the sample.

The characteristic energy $\delta\varepsilon \approx eE\Lambda$ transferred from the electric field to electrons is determined by the magnetic length $\Lambda = (ch/eB)^{1/2}$. In fields around 7 V cm$^{-1}$, which produce inverted oscillations at low generation rates (curve $G_2$ in Fig. 5), $\delta\varepsilon \approx 0.1$ K at $B \approx 40$ kOe, and significant heating can only occur for cold carriers with low kinetic energy $\varepsilon$ in a Landau subband. Therefore, the occurrence of oscillation inversion in relatively weak electric fields, together with its dependence on $T$ (see curve $G_2$), point to cold carriers as dominant contributors to the photocurrent.

All the experimental results presented can be put into a unified framework if we assume that photocurrent peaks at the resonances are observed for the electron distribution function of the Boltzmann form, $f(\varepsilon) = f_0 \exp(-\varepsilon/kT_e)$, in the energy range $\varepsilon \ll \Delta E$ (possibly even with an electron temperature $T_e \neq T$) and that their conversion to troughs occurs when the distribution function becomes strongly non-Boltzmann.

For a Boltzmann function $f(\varepsilon)$, the photocurrent peaks at the resonances are quite naturally explained as being due to an increased concentration of non-equilibrium electrons. Their conversion to troughs may be due to Elesins' [1] mechanism of negative conductivity in crossed electric and magnetic fields in the ultraquantum limit. So our suggested interpretation of the inversion implies that as both the generation rate $G$ and the field $E$ are increased, the distribution function will show a region with $\partial f/\partial\varepsilon > 0$ at small $G$. Although this is a rather difficult point to justify — in particular, because no theoretical calculations are available for processes that determine the function $f(\varepsilon)$ under the specific conditions of our experiments — some qualitative arguments are in order here.

Let us take a look at the electron–phonon coupling first. Because at **B**||[100] the translational motion of electrons in germanium is described by the effective mass $m^* = 1.43m_0$ and the speed of longitudinal sound is $s \approx 5 \times 10^5$ cm s$^{-1}$, we have $m^*s^2 \approx 2.5$ K. The condition

$$m^*s^2 > kT \tag{4}$$

implies that the thermal velocity $v_T = (kT/m^*)^{1/2} < s$, so that thermalized electrons not only cannot emit phonons but are

also somewhat constrained in their ability to absorb phonons. This leads to a greatly reduced electron–phonon energy exchange, which is an extremely important factor because it is precisely the phonon system which acts as a 'sink' for the energy an electron has at the last stage of its thermalization and for the energy it obtains from the electric field. Note that the distribution function remains unaffected by pair electron–electron collisions in the ultraquantum magnetic field limit $\hbar\Omega > \varepsilon$ (see Ref. [14]).

We next turn to experimental arguments and consider the inversion $G_1$ first. The most likely recombination channels are exciton formation and electron capture by $A^+$ centers [15], both of which involve the Coulomb interaction and are therefore the more likely the less $\varepsilon$. Moreover, both are quadratic recombination processes (the latter, at not too low temperatures). Therefore, the concentration of cold carriers is $n_1 \sim G^{1/2}$, whereas for those which are warm and still cooling down we have $n_2 \sim G$. Clearly, as $G$ increases, a point will be reached where the warm electrons outnumber the cool ones; specifically, $n_2 > n_1$ at

$$G > G_1 \approx \tau_c^{-2}\varkappa^{-1}, \tag{5}$$

where $\tau_c$ is the cooling time and the kinetic recombination rate $\varkappa$ is related to the lifetime by $\tau = (\varkappa n_1)^{-1}$. For $G > G_1$, the distribution function may exhibit a maximum at an energy which is determined from the equation $\tau_c(\varepsilon) = \tau(\varepsilon)$ [16].

Clearly, the resulting non-equilibrium distribution can no longer depend on $T$, so that the presence of kinks in the curves in Fig. 6 supports the proposed explanation. (The weak temperature dependence to the left of the kink may be due to changes in the system of scatterers, for example.)

The action of the electric field at generation rates $G \leqslant G_1$ can also be explained from this viewpoint. Heating by the field leads to the same (inversion) effect as lowering the temperature, i.e., $\tau_c$ can be increased both by turning on heating (and thereby decreasing the electron cooling rate) and by lowering the final cooling temperature.

It appears that a somewhat different mechanism actually distorts the distribution function and thereby leads to inversion under the action of an electric field at low generation rates (inversion $G_2$, see Fig. 5). Because of the large value of $m^*s^2$, the way in which electrons with small $\varepsilon$ give off their energy acquired from the field is mainly through electron–exciton or three-electron collisions. If these collisions are too rare due to the low concentration of excitation, then the electric field should lead to the effective depletion of the bottom of the Landau subband.

At large generation rates the electron–electron collisions stabilize the distribution function, 'Boltzmannize' it, and reduce the role of heating to merely moving the effective electron temperature $T_c$ away from the bath temperature $T$, which is the reason why oscillation inversion does not occur until the very moment of breakdown.

The question may be asked here, given that electron–electron collisions are efficient in mixing electrons at $G \sim 10^{17}$ cm$^{-3}$ s$^{-1}$, why do they fail in this task at high pumping rates $G \geqslant G_1$, when the density of excitations is higher? A possible answer is that different energy ranges are of importance in these two cases. While at $G \approx G_2$ the electric field distorts the distribution in the very near vicinity of the subband bottom, at $G \geqslant G_1$ the distortion of the distribution function occurs at $\varepsilon > kT$.

# References

1. Elesin V F *Zh. Eksp. Teor. Fiz.* **55** 792 (1968) [*Sov. Phys. JETP* **28** 410 (1968)]
2. Aleksandrov A S et al. *Zh. Eksp. Teor. Fiz.* **64** 231 (1973) [*Sov. Phys. JETP* **37** 119 (1973)]
3. Kagan Yu *Zh. Eksp. Teor. Fiz.* **38** 1854 (1960) [*Sov. Phys. JETP* **11** 1333 (1960)]
4. Levinson I B *Fiz. Tverd. Tela* **6** 2113 (1964) [*Sov. Phys. Solid State* **6** 1665 (1965)]
5. Yamada E, Kurosawa T *J. Phys. Soc. Jpn.* **34** 603 (1973)
6. Ryzhiĭ V I *Zh. Eksp. Teor. Fiz.* **64** 643 (1973) [*Sov. Phys. JETP* **37** 327 (1973)]
7. Mani R G et al. *Nature* **420** 646 (2002); Zudov M A et al. *Phys. Rev. Lett.* **90** 046807 (2003); Yang C L et al. *Phys. Rev. Lett.* **91** 096803 (2003); Dorozhkin S I *Pis'ma Zh. Eksp. Teor. Fiz.* **77** 681 (2003) [*JETP* **77** 577 (2003)]; Willett R L, Pfeiffer L N, West K W *Phys. Rev. Lett.* **93** 026804 (2004)
8. Dorozhkin S I *Pis'ma Zh. Eksp. Teor. Fiz.* **77** 681 (2003) [*JETP* **77** 577 (2003)]; Dmitriev I A et al., cond-mat/0310668; Dietel J et al., cond-mat/0407298
9. Gantmakher V F, Zverev V N *Zh. Eksp. Teor. Fiz.* **71** 2314 (1976) [*Sov. Phys. JETP* **44** 1220 (1976)]
10. Gantmakher V F, Zverev V N, in *Landau Level Spectroscopy* Vol. 2 (Modern Problems in Condensed Matter Sci., Vol. 27.2, Eds G Landwehr, E I Rashba) (Amsterdam: North-Holland, 1991) p. 1135
11. Gantmakher V F et al. *Izv. Akad. Nauk SSSR, Ser. Fiz.* **42** 1160 (1978); Gantmakher V F, Zverev V N, Shovkun D V *Fiz. Tekh. Poluprovodn.* **22** 575 (1988)
12. Gantmakher V F, Zverev V N *Zh. Eksp. Teor. Fiz.* **69** 695 (1975) [*Sov. Phys. JETP* **42** 352 (1977)]
13. Zverev V N *Fiz. Tverd. Tela* **19** 2015 (1977)
14. Kogan Sh M, Shadrin V D, Shul'man A Ya *Zh. Eksp. Teor. Fiz.* **68** 1377 (1975) [*Sov. Phys. JETP* **41** 686 (1975)]
15. Gershenzon E M, Ladyzhinskiĭ Yu P, Mel'nikov A P *Fiz. Tekh. Poluprovodn.* **7** 1100 (1968)
16. Ladyzhinskiĭ Yu P *Fiz. Tverd. Tela* **11** 2282 (1969) [*Sov. Phys. Solid State* **11** 1842 (1969)]

# Microwave-induced negative conductivity and zero-resistance states in two-dimensional electronic systems: history and current status

V I Ryzhiĭ

## 1. Introduction

The history of the effect of absolute negative conductivity in semiconductor structures and its current studies are briefly reviewed here. We focus primarily on this effect in two-dimensional electron systems in a magnetic field under microwave radiation in the context of the so-called zero-resistance, as well as zero-conductance, states observed in recent experiments.

The possibility of realizing negative dc conductivity in a non-equilibrium electron system, i.e., the situation when the dc current $\mathbf{J}$ flows in the direction opposite to the direction of the electric field $\mathbf{E}$, was qualitatively discussed for the first time by Krömer in the late 1950s [1] in connection with his proposal of negative electron mass. In such a situation, the usual dc conductivity $\sigma_{\mathrm{D}} = \mathbf{JE}/E^2 < 0$, so that one can say that we have to deal with the effect of absolute negative conductivity (ANC). This effect should be distinguished from the effect of negative differential conductivity (NDC) which occurs in many semiconductor structures, in particular in Gunn diodes. Different realistic mechanisms of ANC in two- and three-dimensional electron systems (2DESs and 3DESs, respectively) in which a substantial deviation from equilibrium is associated with intraband or interband absorption of optical radiation were considered more than three decades ago [2 – 7] (see also Ref. [8]). A mechanism of ANC in a 2DES subjected to a magnetic field and irradiated with microwaves was first proposed by the author [9]. This mechanism is related to 2D electron scattering by impurities accompanied by the absorption of microwave photons. It was shown that the dissipative dc conductivity (the diagonal component of the conductivity tensor) is an oscillating function of the ratio of the microwave frequency $\Omega$ to the electron cyclotron frequency $\Omega_{\mathrm{c}} = eH/mc$, where $e = |e|$ and $m$ are the electron charge and effective mass, $H$ is the magnetic field strength, and $c$ is the speed of light. At $\Omega$ somewhat exceeding $\Omega_{\mathrm{c}}$ or a multiple of $\Omega_{\mathrm{c}}$, the photon-assisted impurity scattering of 2D electrons with their transitions between the Landau levels (LLs) results in a contribution to the dissipative current flowing opposite to the electric field. At sufficiently strong microwave radiation, this scattering mechanism can dominate, leading to ANC when $\Omega \geqslant \Lambda\Omega_{\mathrm{c}}$, where $\Lambda = 1, 2, 3, \ldots$. Possible transformation of the current – voltage characteristic of a 2DES with increasing microwave power $P$ is schematically shown in Fig. 1.

There were several early but unsuccessful attempts to observe experimentally the effect of ANC associated with the mechanisms in question, although some features of the transport phenomena in 3DESs and 2DESs studied at that time can be attributed to these mechanisms. Early theoretical and experimental studies related to ANC have been eclipsed by the discovery of the integral and fractional quantum Hall effects and very extensive related activities.

Recently, Mani et al. [10] and Zudov et al. [11] have observed experimentally the effect of vanishing electrical resistance (in the Hall bar configuration) in high-quality 2DESs (with electron mobility on the order of $\mu \sim 10^7$ cm$^2$ V$^{-1}$ s$^{-1}$) at low temperatures ($T \sim 0.1$ K) in rather weak magnetic fields ($H \sim 0.1$ T) irradiated with microwaves (with frequencies $f = \Omega/2\pi$ in the range of several tens of GHz). The obtained experimental magnetic-field dependences of the longitudinal resistance $R_{xx}$ are shown in Fig. 2 [10, 11]. As shown, in the presence of sufficiently strong microwave radiation, $R_{xx}$ vanishes in some ranges of the magnetic field. Due to an association
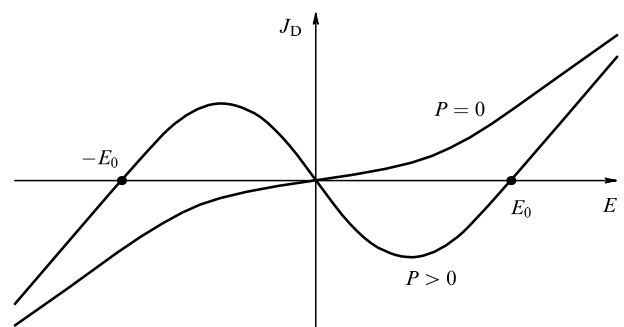
**Figure 1.** Schematic view of current – voltage characteristics without ($P = 0$) and with ($P > 0$) microwave radiation.